Inorganic Chemistry

Article

pubs.acs.org/IC

Symmetrical Hydrogen Bonds in Iridium(III) Alkoxides with Relevance to Outer Sphere Hydrogen Transfer

Nathan D. Schley,[†] Stéphanie Halbert,[‡] Christophe Raynaud,[‡] Odile Eisenstein,[‡] and Robert H. Crabtree*[,†]

[†]Department of Chemistry, Yale University, P.O. Box 208107, New Haven, Connecticut 06520-8107, United States

[‡]Institut Charles Gerhardt, UMR 5253 CNRS, Université Montpellier 2, cc 1501, Place Eugène Bataillon Montpellier, 34095, France

Supporting Information

ABSTRACT: A chelating ligand formed by deprotonation of 2-(2′-pyridyl)-2-propanol stabilizes a distorted trigonal bipyramidal geometry in a 16e$^-$ d^6 5-coordinate iridium complex with the alkoxide acting as a π donor. Ambiphilic species such as AcOH bearing both nucleophilic and electrophilic functionality form adducts with the unsaturated iridium complex which contain strong intramolecular O···H···O hydrogen bonds that involve the basic alkoxide oxygen. Density functional theory (DFT) calculations on the isolated cations reproduce with high accuracy the geometrical features obtained via X-ray diffraction and corroborate the presence of very short hydrogen bonds with O···O distances of about 2.4 Å. Calculations further confirm the known trend that the hydrogen position in these bonds is sensitive to the O···O distance, with the shortest distances giving rise to symmetrical O···H···O interactions. Dihydrogen is shown to add across the Ir−O π bond in a presumed proton transfer reaction, demonstrating bifunctional behavior by the iridium alkoxide.

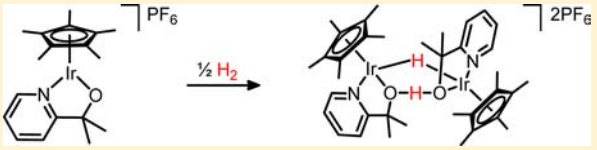

INTRODUCTION

Alkoxides are common ligands in transition metal chemistry and frequently encountered in homoleptic alkoxide complexes[1,2] or as intermediates in hydrogen-transfer and C−O bond-forming catalysis. Reactions of metal alkoxides typically reflect their nucleophilicity and basicity, though metal alkoxides with a β hydrogen atom often decompose by β-hydride elimination. For this reason, tertiary alkoxides and phenoxides are an important subclass of alkoxides that are more likely to give rise to stable metal alkoxide complexes owing to their inability to undergo β-hydride elimination. The oxophilicity of early transition metal complexes is well-known and stems in part from the favorable overlap of oxygen lone pairs with empty metal d_π orbitals. Alkoxide complexes of the late transition metals[3] such as iridium[4] are less common, reflecting their increased electronegativity. In addition, the presence of filled d_π orbitals in d^8 square planar and d^6 octahedral geometries leads to repulsive interactions with the ligand lone pairs.[5]

In certain cases however, unsaturated late transition metal complexes can be isolated in unusual geometries owing to a stabilizing effect of ligand π electron overlap with empty metal d orbitals.[5] For instance, the 18e$^-$ Ru^{II} complex CpRuCl(1,2-bis(diphenylphosphino)propane) undergoes halide exchange by a dissociative mechanism via a 16e$^-$ 5-coordinate pyramidalized intermediate and a distorted trigonal bipyramidal transition state.[6] The π basic alkoxide ligand in a related half-sandwich complex, Cp*Ru(OCH_2CF_3)(PCy_3), allows isolation of a stable distorted trigonal bipyramidal (DTBP) 16e$^-$ complex.[7] Likewise, the entire family of Cp*RuLX complexes (L = $^iPr_3$, X = Cl, Br, I, OCH_2CF_3, $OSiPh_3$, $OSiMe_2Ph$, NHPh) have been shown to adopt the same distorted trigonal bipyramidal geometry in which the L and X ligands, ruthenium atom, and Cp* centroid are coplanar (Figure 1).[8] Very bulky

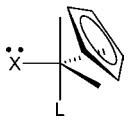

Figure 1. Distorted trigonal bipyramidal (DTBP) geometry supported by π donor ligand X.

ancillary ligands appear to stabilize 5-coordinate DTBP species with weak π donor ligands such as chloride,[9] and on at least one occasion a DTBP Cp*Ru complex lacking a π donor ligand has been characterized, though its X-ray crystal structure shows some distortion toward a pyramidal geometry.[10] Anionic nitrogen ligands play a similar role to π basic alkoxides, including in low coordination-number Cp*Ir imido species prepared and studied by Bergman.[11]

Unsaturated metal complexes having ligand−metal multiple bonds often display unusual reactivity including addition reactions across the metal−ligand π bonds and ligand bifunctionality.[12] In particular, the addition of hydrogen across a ruthenium-amido double bond to give a hydridoruthenium amine complex plays an important role in bifunctional, outer-sphere hydrogenation catalysis.[13] This is believed to occur via a proton transfer reaction from a dihydrogen complex to a basic acceptor ligand.[12,14,15] The corresponding addition of dihy-

Received: July 22, 2012
Published: October 29, 2012

drogen across a metal-alcoholate double bond to give a metal hydride and alcohol ligand is clearly plausible, and may occur in certain systems,[16] but has not yet been demonstrated to the best of our knowledge. Alkoxide complexes of late transition metals known to form strong metal-hydrides are the most likely candidates for dihydrogen addition across a metal−oxygen π bond, a pathway which could have implications in hydrogenation catalysis.[17]

The preparation and coordination chemistry of a DTBP cationic Ir^{III} alkoxide is reported here with a focus on the role of the oxygen π electrons in determining the geometry and reactivity of the complex and derivatives containing strong, short intramolecular hydrogen bonds. Strong hydrogen bonds with symmetrical O···H···O structures are not common, but when they occur are associated with short O···O distances of around 2.4 Å and with the proton acceptors having anionic character.[18] Localization of the proton is difficult by X-ray diffraction and so computational support is often needed.[19,20]

In addition to spectroscopic and crystallographic data, density functional theory (DFT) calculations have been carried out to further describe the nature of the bonding in these cationic alkoxides. A number of prior computational studies have examined the relationship between the structure (distance between the proton donor and the proton acceptor) and both the strength of the hydrogen bond and the deshielding of the associated proton.[21−26] For this study the available crystal structures were used as an initial guess for geometry optimization. This was carried out for the isolated cations leading in all cases to excellent agreement between calculated and experimental structures and fair agreement between calculated and experimental ^{1}H NMR chemical shifts. Inclusion of the explicit counteranion worsens the agreement. Because this work is focused on the interactions within the metal species, calculations with explicit anions are not discussed here. For convenience, computational results for each species follow the presentation of the experimental results.

RESULTS

In a recent report, the reaction of 2-(2′-pyridyl)-2-propanol with $[Cp^*IrCl_2]_2$ in the presence of sodium bicarbonate was shown to give a neutral Ir^{III} alkoxide complex: Cp*IrCl(2-(2′-pyridyl)-2-propanolate) (**1**[**Cl**]). Subsequent anion metathesis with silver trifluoroacetate gave Cp*Ir(trifluoroacetate)(2-(2′-pyridyl)-2-propanolate) which adopts a solid-state structure in which the trifluoroacetate anion is bound inner-sphere.[27] Substitution of silver trifluoroacetate for silver hexafluorophosphate gives **1**[$\mathbf{PF_6}$], which can be prepared more-conveniently in one step without the use of a silver salt by the reaction of 2-(2′-pyridyl)-2-propanol with $[Cp^*IrCl_2]_2$ and potassium hexafluorophosphate under basic biphasic conditions (Scheme 1). The product Cp*Ir(2-(2′-pyridyl)-2-propanolate)PF_6 (**1**[$\mathbf{PF_6}$]) is obtained directly from the organic phase as an air-stable red solid after evaporation of the solvent. Single-crystal X-ray diffraction shows that **1**[$\mathbf{PF_6}$] adopts a distorted trigonal bipyramidal geometry with the chelating alkoxide ligand orthogonal to the plane containing the Cp* ligand (Figure 2, left). This geometry is comparable to that of several known Cp*Ir dialkoxides[28−30] and is presumed to be stabilized by donation of oxygen π electrons into a vacant metal d orbital orthogonal to the plane containing the pyridyl ligand. The Ir−O bond is 1.942(4) Å which is consistent with some double bond character and indeed is among the shortest iridium-alkoxide bonds known.[31] **1**[$\mathbf{BPh_4}$] obtained in a similar manner to **1**[$\mathbf{PF_6}$] adopts the same geometry and a comparable Ir−O bond distance of 1.937(3) Å.

The calculated structure of the isolated cation **1**, denoted **1-T**, is essentially identical to that observed experimentally for **1**[$\mathbf{PF_6}$] (Figure 4). The metal is coplanar with the cyclopentadienyl centroid and the oxygen and nitrogen atoms, such that the two methyl groups on the 2-pyridyl-2-propanolate ligand are equivalent. The calculated Ir−O bond distance of 1.921 Å is marginally shorter than the experimental distance of 1.942(4) Å, and the calculated Ir−N bond distance of 2.075 Å is slightly longer than the experimental distance of 2.057(4) Å. The preference for planarity at the metal is due to the presence of a d_π-p_π Ir−O interaction similar to that found for $Cp^*Ru^{II}XL$ complexes in which the ligand X donates π electrons to a vacant metal d orbital.[8]

Adduct Formation with Lewis Bases. Despite the oxygen to iridium π donation, **1** is still coordinatively unsaturated, which implies that it should form adducts with Lewis-basic ligands (Figure 3). Binding of a Lewis base disrupts the d_π-p_π interaction; therefore the stability of adducts of **1** is determined mainly by the energy difference between the oxygen π donation in **1** and the new bonds in the adduct. Although dichloromethane solutions are deep red, solutions of **1**[$\mathbf{PF_6}$] in methanol and acetonitrile are orange and yellow, respectively, though evaporation of these solutions gives **1**[$\mathbf{PF_6}$] back quantitatively. This is consistent with the formation of reversible adducts with these ligating solvents. On one occasion, storage of a concentrated methanolic solution of **1**[$\mathbf{PF_6}$] at −20 °C for an extended period of time gave several large orange crystals of the methanol adduct [**1·MeOH**]$\mathbf{PF_6}$ which could be characterized by X-ray crystallography; however, the crystals were not stable at room temperature and rapidly desolvated. (Figure 2, right) The crystallization of [**1·MeOH**]$\mathbf{PF_6}$ could not be reproduced reliably. It is clear, however, that methanol binds only weakly to **1**, as the ^{1}H NMR spectrum of **1**[$\mathbf{PF_6}$] at −60 °C in MeOD-d_4 shows no evidence of decoalescence of the geminal methyl groups of the pyridylpropanolate ligand. Under these conditions, rapid exchange between octahedral [**1·MeOH**]$\mathbf{PF_6}$ and DTBP **1**[$\mathbf{PF_6}$] makes the two methyl groups equivalent.

1[$\mathbf{PF_6}$] reacts with carbon monoxide in methanol to give the cationic iridium carbonyl complex **2**. (Figure 5) Carbonyl binding appears to be weak and reversible, as sparging solutions of **2** with argon gas causes the regeneration of **1**[$\mathbf{PF_6}$]. Accordingly, the carbonyl stretching frequency of **2** is 2039 cm^{-1}, consistent with weak backbonding by the cationic Ir^{III} metal center. Labilization of carbonyl ligands by cis ligands having lone pairs is a known phenomenon, and likely contributes to the instability of **2** in solution.[5] In the solid state, the carbonyl C−O bond length is 1.136(7) Å, in very good agreement with a similar cationic Ir^{III} carbonyl complex $[Cp^*Ir(\kappa^2(N,C)\text{-}\{NH_2C(CH_3)_2\text{-}2\text{-}C_6H_4\}(CO)]BF_4$ [ν(CO) = 2036 cm^{-1} and C−O = 1.135(4) Å].[32]

Scheme 1. Preparation of 1[$\mathbf{PF_6}$]

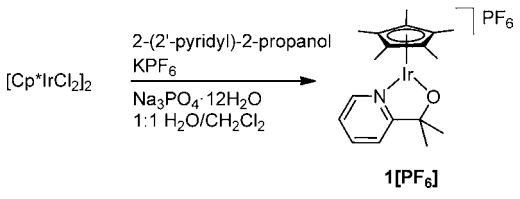

dx.doi.org/10.1021/ic301601c | Inorg. Chem. 2012, 51, 12313−12323

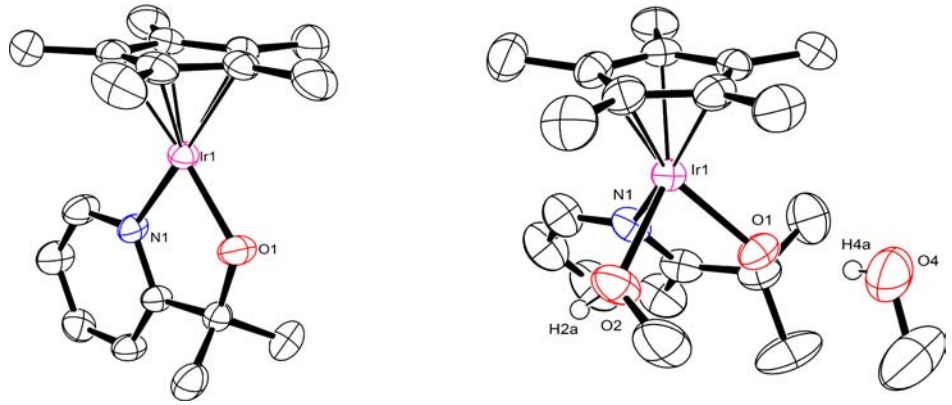

Figure 2. ORTEP diagrams of **1**[PF_6] (left) and [**1·MeOH**]PF_6 (right) shown at 50% probability. Anions and some solvent molecules have been omitted for clarity.

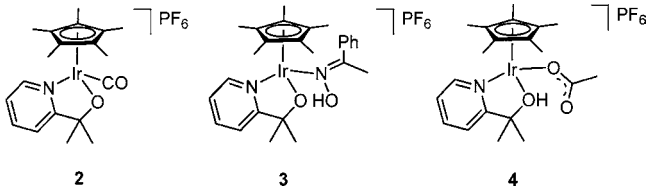

Figure 3. Complexes **2**, **3**, and **4**.

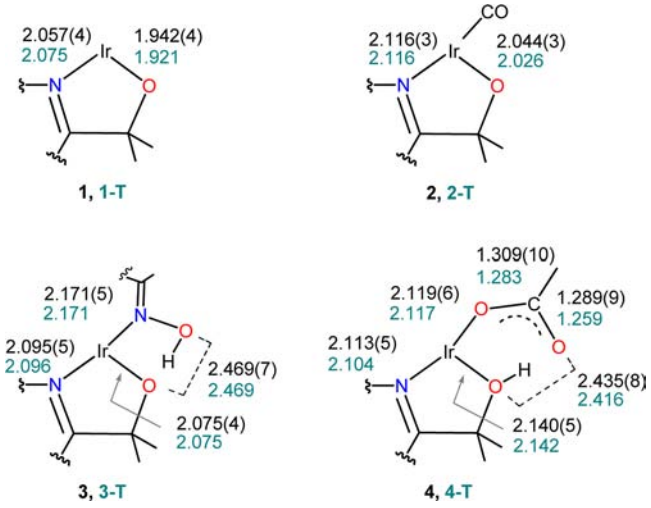

Figure 4. Selected bond lengths (Å). Experimental values are presented in black, calculated values in teal.

The calculated structure of the isolated cation of **2**, denoted **2-T**, gives a C−O bond distance of 1.151 Å, an Ir−O bond distance of 2.026 Å and an Ir−N bond distance of 2.116 Å (Figure 4). The values for the Ir−O and Ir−N bonds are in remarkable agreement with the experimental distances of 2.044(3) and 2.116(3) Å, respectively. The presence of the carbonyl ligand and the change to an octahedral geometry lengthens both the Ir−O and the Ir−N bonds relative to **1** with the former being lengthened more (Δ_{exp} = 0.102(5), Δ_{calc} = 0.105 Å) than the latter (Δ_{exp} = 0.059(5) Å, Δ_{calc} = 0.041 Å). The effect of CO coordination on the Ir−O bond is in large part due to the loss of the Ir−O d_{π}-p_{π} bonding, though the change in the Ir−N bond distance suggests that σ bonds are also influenced. The calculated ν(CO) stretching frequency in **2-T** is shifted to lower frequency by 92 cm^{-1} relative to free CO, which is also in fair agreement with the experimental red shift of 104 cm^{-1} measured in the solid state, confirming that the cationic Ir^{III} center is capable of weak backbonding. Overall, the interaction between **1** and CO is represented in a reasonably quantitative manner by the DFT calculations.

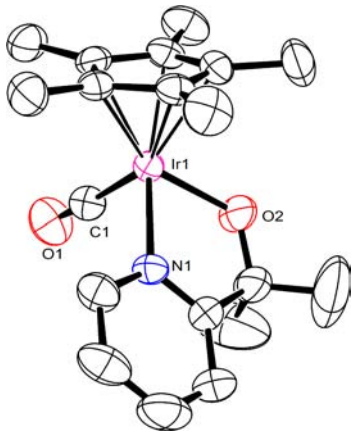

Figure 5. ORTEP diagram of **2** shown at 50% probability. Anion and solvent have been omitted for clarity.

Adduct Formation Involving Intramolecular H-Bonds. The unsaturated structure of **1** and the Lewis basicity of the alkoxide ligand present an interesting opportunity for inner and secondary coordination sphere interactions with ligands that present both a Lewis acidic and basic site. The reaction of **1**[PF_6] with acetophenone oxime gives the adduct **3** (Figure 3). The ^{1}H NMR spectrum of **3** shows a very low field resonance for the oxime proton at +14.9 ppm that is shifted substantially from the oxime signal of free acetophenone oxime which typically appears near 9 ppm in $CDCl_3$.[33,34] Single crystal X-ray diffraction confirms that the acetophenone oxime ligand is hydrogen bonded to the pyridylpropanolate ligand with an O···O distance in the solid state of 2.469(7) Å (Figure 6, left). There is also a 3 Å close contact between oxime oxygen atoms of neighboring molecules of **3**, which may introduce some hydrogen bond disorder.

The geometry optimization of the cation of **3**, denoted **3-T**, gives Ir−O, Ir−$N_{pyridine}$, and Ir−N_{oxime} bond distances of 2.075, 2.096, and 2.171 Å, respectively, which compare very well with the corresponding experimental values (Figure 4). The calculated distance between the oxygen atoms of the pyridylpropanolate ligand and the oxime is identical (2.469 Å) to that obtained in the crystal structure, and the proton is

dx.doi.org/10.1021/ic301601c | Inorg. Chem. 2012, 51, 12313−12323

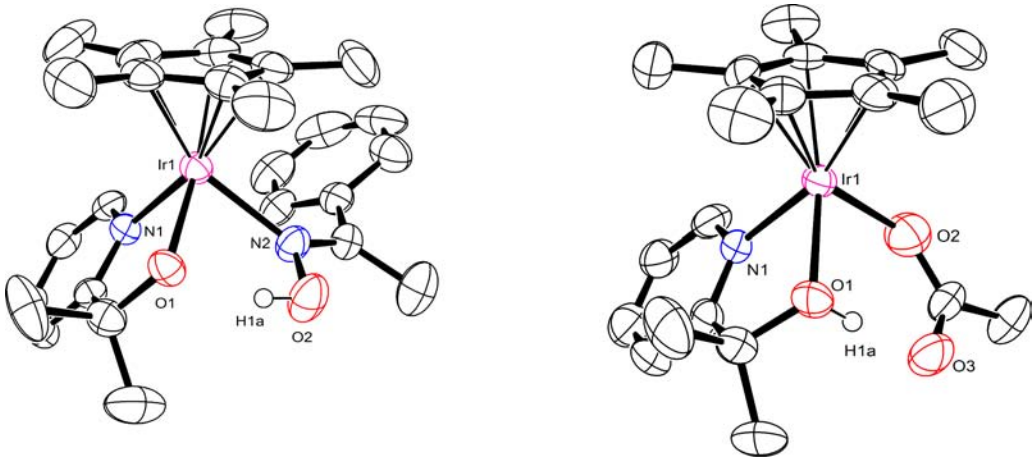

Figure 6. ORTEP diagrams of **3** (left) and **4** (right) shown at 50% probability. Anions have been omitted for clarity.

calculated to be 0.864 Å from the oxime oxygen and 1.679 Å from the pyridylpropanolate oxygen. The open O···HO angle of 150.8° is consistent with a hydrogen bond between these two oxygen atoms. The elongation of the Ir−$O_{alkoxide}$ bond in **3** is part of a trend from **1** to **2** to **3** which suggests that the Ir−$O_{alkoxide}$ distance is a sensitive reporter of both ligand−metal and intramolecular ligand−ligand interactions involving the pyridylpropanolate oxygen atom. The calculated deshielding of the proton is +15.9 ppm, similar to the experimental value of +14.9 pm observed in solution. The geometry of **3-T** illustrates the ability of **1** to interact with ambiphilic species having both nucleophilic and electrophilic functionality by addition across the formal Ir−O π bond of **1**, with the Lewis acid interacting with the propanolate and the Lewis base with the iridium center. These interactions can be described as bifunctionality in the Ir−O π bond and are further explored below.

1[PF_6] reacts with acetic acid to form an adduct **4** in which the proton from acetic acid is shared by the chelate ligand and the acetate ion, which is bound to iridium through a single oxygen atom (Figure 6, right). The proton could not be located by X-ray crystallography, but at −60 °C a resonance in the ^{1}H NMR corresponding to the proton of interest could be found at +15.77 ppm. The resonance is shifted downfield from a typical hydrogen bonded carboxylic acid and along with the very short O···O distance of 2.435(8) seen in the X-ray structure, is consistent with a strong hydrogen bond between the protonated ligand and the acetate.

The calculated structure of **4**, denoted **4-T**, is very similar to the solid-state structure as shown by the selected distances in Figure 4. The 5-membered ring containing the iridium atom, the central carbon, and two oxygen atoms of the acetate, and the ligand oxygen atom O1 (Figure 6, right) has the shape of a flattened envelop with the largest dihedral angle being 16°. Calculations show that the proton is closer to the propanolate oxygen O1 than to the O3 atom of the acetate (O1−H = 1.098 Å, O3···H = 1.327 Å). This is consistent with protonation to give a pyridylpropanol ligand, which is also seen in the elongated Ir−O1 bond of 2.142 Å (exp: 2.140(5) Å), the longest such bond in the family of complexes characterized by crystallography here.

The calculated O1···O3 distance of 2.416 Å is marginally shorter than the experimental value of 2.435(8) Å. These values are indicative of a strong hydrogen bond, which is further evidenced by the deshielding of the proton involved in the O···HO interaction. The calculated chemical shift of +19.7 ppm is larger than the experimental chemical shift of +15.77 ppm. While the calculations of ^{1}H NMR chemical shifts in **3-T** and **4-T** do not reproduce the experimental values, they accurately predict that the deshielding is larger in **4** than in **3**.

The reaction of **1** with substoichiometric hydrogen chloride most conveniently introduced by addition of 0.5 equiv of diphenylammonium chloride[35] gives complex **5**, a dicationic diiridium salt composed of two iridium fragments bridged by a chloride and by an OH···O hydrogen bond in which the two proximal ligands share a proton (Scheme 2). The experimental

Scheme 2. Preparation of 5 from 1[PF_6]

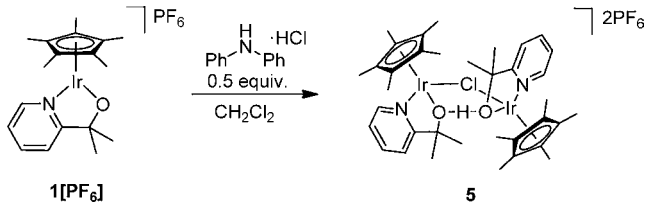

1[PF_6] 5

O···O distance from the X-ray crystal structure is 2.452(10), as shown in Figure 8, and is substantially shorter than a related diiridium chloro-bridged pyrazole-pyrazolate complex with similar geometry (N···N = 2.736(10)).[35] The Shvo dimer[36] is the best known dimeric metal alcohol−alcoholate, though other examples with short O···O distances have been reported.[37,38] More generally, alcohol−alcoholate interactions are common drivers of packing in the solid state for complexes containing multiple alcohol or alcoholate ligands in mixed protonation states.[39]

The geometry optimization of the dication **5**, denoted **5-T**, gives a structure that is in very good agreement with the solid state structure (Figure 7). A computational search for isomeric structures differing by the relative orientations of the two metal fragments and the presence or the absence of the OH···O interaction did not locate other minima, suggesting that the experimentally observed geometry is the lowest energy isomer.

Full details of the optimized structure are given in the Supporting Information; however, we focus here on the chloride and OH···O bridges. The optimization gives a structure with the hydrogen of the OH···O unit bonded in a nonsymmetrical manner to the two oxygen atoms with OH distances of 1.093 and 1.367 Å. This dissymmetry is associated with one of the propanolate ligands being protonated, with a

dx.doi.org/10.1021/ic301601c | *Inorg. Chem.* 2012, 51, 12313−12323

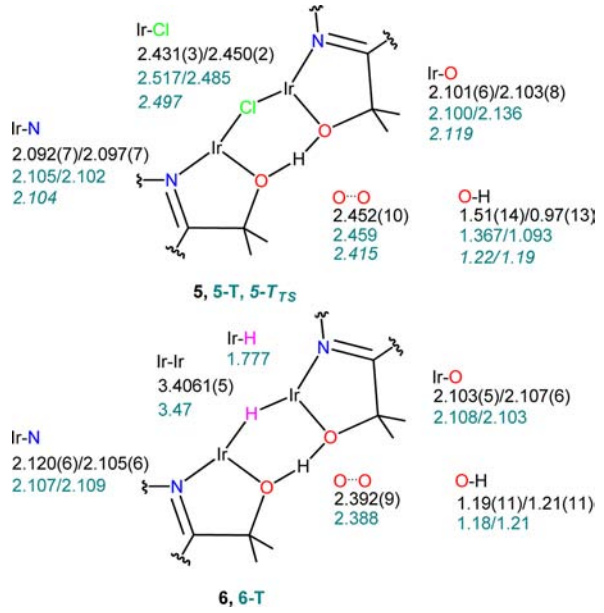

Figure 7. Selected bond lengths (Å). Experimental values are presented in black, calculated values for **5**/**6-T** in teal, and calculated values for **5-T**$_{TS}$ (the transition state for H^+ exchange, 1.4 kcal mol^{-1} above **5-T**) in teal and italics.

shorter Ir−O bond in the nonprotonated pyridylpropanolate ligand (2.100 Å vs 2.136 Å). The Ir−Cl−Ir bridge is also unsymmetrical, with the bridging chloride being closer to the iridum bonded to the pyridylpropanol ligand (Ir_{ol}-Cl = 2.485 Å) than the propanolate ligand (Ir_{olate}-Cl = 2.517 Å). The calculated distance between the two oxygen atoms is 2.459 Å. The iridium, chlorine, and oxygen atoms are approximately coplanar, with the greatest deviation from the calculated average plane being 0.270 Å and involving the oxygen atoms.

Despite the unsymmetrical nature of the located minimum, **5-T**, the transition state for proton exchange between the two oxygen atoms, **5-T**$_{TS}$, is found to be 1.4 kcal mol^{-1} (including ZPE correction) above **5-T**. This small difference in energy indicates a low-barrier hydrogen bond which cannot really be distinguished from a symmetrical minimum.[40] These results show that the proton is essentially delocalized between the two oxygen atoms. The calculated transition state for hydrogen exchange, **5-T**$_{TS}$, can be considered as representative of the average symmetrical structure.

The bond distances in **5-T** and **5-T**$_{TS}$ are compared in Figure 7, and differ primarily in the overall symmetry of the molecule, with **5-T**$_{TS}$ having symmetrical Ir−O and Ir−Cl distances and a shorter overall O···O distance. The crystal structure of **5** is more similar to **5-T**$_{TS}$ than **5-T**; however, the experimental O···O distance is closer to that found in **5-T**. The calculated ^{1}H NMR chemical shift of the OH···O proton is +16.6 for the nonsymmetrical structure **5-T** and +17.5 ppm for **5-T**$_{TS}$. Both values are substantially higher than the experimental value of +14.24 ppm but are in line with the overestimated deshielding calculated for **3-T** and **4-T**.[41]

Addition of H_2 Across an Ir−O π Bond. The reactions of **1**[PF_6] with acetic acid and diphenylammonium chloride to give **4** and **5**, respectively, illustrate the ability of acids HX (X = OAc, Cl) to add across the Ir−O π bond in **1**. It therefore seemed possible that an analogous reaction might occur with hydrogen to give the protonated ligand and an iridium hydride, provided that dihydrogen was sufficiently acidified by ligation to the iridium center. Indeed, **1**[PF_6] reacts slowly with H_2 in methylene chloride-d_2 at room temperature to give a new set of ^{1}H NMR signals including a downfield resonance at +16.14 and an upfield resonance at −15.00 ppm. This new product cannot be obtained in pure form under these conditions; however, optimization of the hydrogenation of **1**[PF_6] revealed that **6** could be obtained as an orange crystalline product by hydrogenation in methanol at low temperatures followed by removal of the solvent. (Scheme 3) Single crystal X-ray

Scheme 3. Partial Hydrogenation of 1[PF_6] to Give the Dimeric Product 6

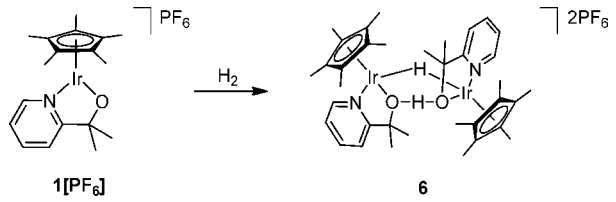

diffraction of crystals of **6** show a dimeric structure comparable to **5** in which heterolysis of H_2 provides a bridging hydride and the proton for the OH···O bridge (Figure 8, right). The OH···O proton could be located in the difference density map and was refined without restraint to a final position equidistant between the two oxygen atoms (OH distances of 1.21(11) Å and 1.19(11) Å).[42] While there is structural similarity between **5** and **6**, the hydride bridge in **6** constrains the dimer such that it crystallizes with a short 3.4 Å distance between the iridium atoms, approximately 1 Å shorter than the separation between the iridium centers in **5**.

^{1}H NMR spectra of a pure solution of **6** could be obtained by dissolution of **6** in DCM-d_2 prechilled to −78 °C, and transferring the cold tube to an NMR instrument at −60 °C. At this temperature the 30:1 ratio of the Cp* protons to the downfield proton and upfield hydride resonances confirm the dimeric structure seen in the solid state. Warming the sample to 0 °C causes the appearance of a new product in the ^{1}H spectrum that does not revert if the sample is cooled again, which suggests that the stability of **6** in solution is limited. The signals corresponding to **6** are still discernible after several hours at room temperature, but **1** is present as a major product, presumably by loss of hydrogen from **6**. In contrast, **6** is stable in the solid state in air for months.

If **1**[PF_6] is treated with H_2 for an extended period of time, over-reduction occurs to give the dimeric hydride [$(Cp^*Ir)_2(\mu$-$H)_3$]PF_6 with dissociation of the protonated ligand 2-(2′-pyridyl)-2-propanol. Related behavior has been observed previously for Cp*Ir complexes of 2-pyridonate ligands,[43,44] and is likely related to the stability of the hydride-bridged Cp* Ir dimers, the reactivity of which has been studied in detail by Maitlis and Bergman.[45−49] The monomeric product of addition of H_2 to **1**[PF_6] would be **7**, a likely product of further hydrogenation of the dimer **6** and a plausible intermediate to over-reduced products such as [$(Cp^*Ir)_2H_3$]PF_6 (Scheme 4). Attempts to prepare **7** by careful hydrogenation of **1**[PF_6] revealed that the reaction of H_2 with **1**[PF_6] is strongly solvent-dependent and does not occur in dimethylsulfoxide or acetonitrile. However, treatment of **1**[PF_6] in DMF-d_7 with H_2 for 30 min causes the appearance of a new product with an upfield proton resonance at −7.41 ppm and a downfield resonance at +10.58 ppm in the ^{1}H NMR spectrum. On the

dx.doi.org/10.1021/ic301601c | Inorg. Chem. 2012, 51, 12313−12323

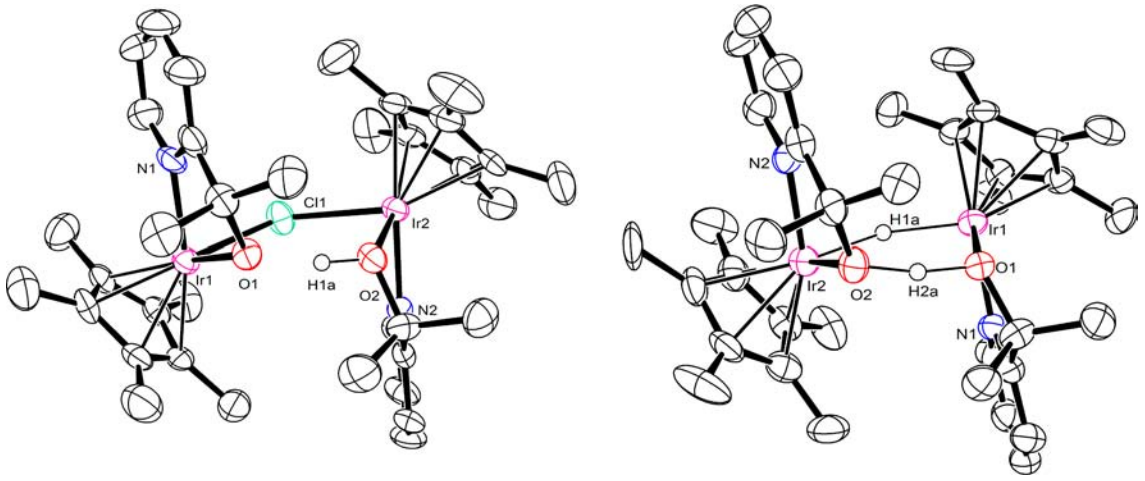

Figure 8. ORTEP diagrams of **5** (left) and **6** (right) shown at 50% probability. Anions and solvent have been omitted for clarity.

Scheme 4. Plausible Pathway for Formation of the Monomer 7 via Dimer 6

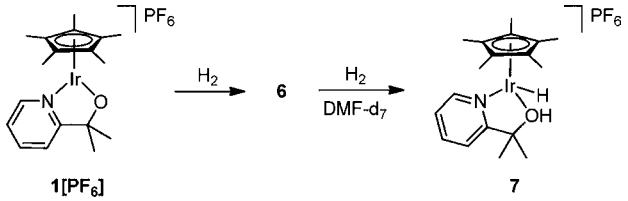

basis of their integrations relative to ligand resonances, this is presumed to be the monomeric product **7**. The lifetime of **7** in solution is limited and it could not be isolated in the solid state, as attempts at crystallization typically gave the dimer **6**.

Calculations on the dimeric dication of **6**, denoted **6-T**, give a structure that is in good agreement with the experimental solid state structure (Figure 7). The iridium-hydride bond distances are identical and calculated to be 1.777 Å, enforcing a short distance between the two metal fragments. Consequently, the calculated O···O distance of 2.388 Å is the shortest such distance in this work and is associated with an essentially symmetrical hydrogen bond with O···H distances of 1.182 and 1.209 Å. This symmetrical H bonding leads to equal Ir−O bond distances of 2.108 Å, which is in good agreement with the experimental values of 2.103 (5) and 2.107(6). The 6-membered ring containing the iridium and oxygen atoms and the proton and hydride is nearly flat, having a deviation of atoms from the average plane of less than 0.2 Å. The calculated ^{1}H NMR chemical shifts for the hydride and proton are found to be −5.8 and +15.9 ppm respectively. The downfield shift of the proton is well reproduced (δ_{exp}: +16.1 ppm), and the agreement is better than in the previously described complexes. However, the chemical shift calculated for the hydride is significantly different from the experimental value. Chemical shifts of metal hydrides are challenging to reproduce,[50,51] and quantitative reproduction of this value is not the topic of this study. Since the geometry of this dicationic dimer is likely rather rigid, it is not surprising that the downfield shift of the bridged proton is well reproduced.

Although **7**, the presumed monomeric product of H_2 addition to **1** could not be isolated, calculations provide a means to analyze its likely structure, denoted **7-T** (Figure 9, right). The isomer in which the hydride and proton are synperiplanar is preferred over the antiperiplanar isomer by 1.9

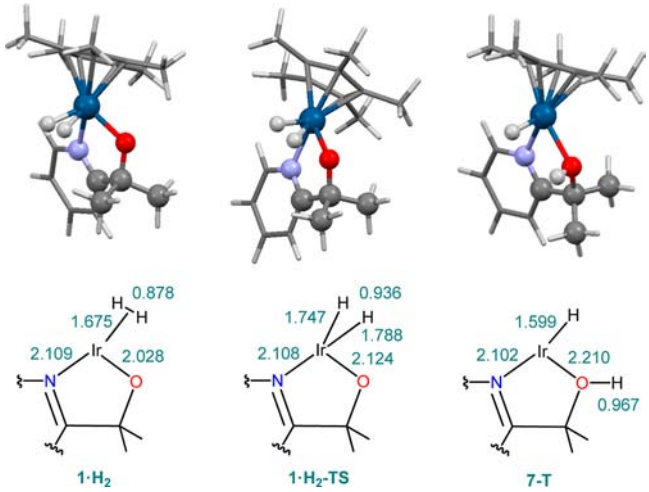

Figure 9. Optimized extrema in the hydrogenation of **1**. Distances in Å.

kcal mol^{-1}. The optimized cation **7-T** has the expected structure of an 18 e$^-$ half-sandwich complex, with Ir−N and Ir−O bonds of 2.102 Å and 2.210 Å, respectively. The calculated Ir−O length is the longest of all species presented here. The ^{1}H chemical shift of the hydride is calculated to be −0.8 ppm while the proton is calculated to be +3.4 ppm. These values deviate substantially from experimental values; however, the proton resonance is expected to shift substantially when involved in a hydrogen bonding interaction. Thus it is likely that the experimentally observed proton resonance is greatly influenced by hydrogen bonding with the solvent.

The energy profile for the hydrogenation of **1** was explored computationally. The reaction begins with coordination of H_2 to give the dihydrogen adduct **1·H$_2$** (Figure 9, left). While the H_2 adduct is calculated to be a local minimum, its energy is 9.6 kcal mol^{-1} higher than that of **1** and free H_2 even prior to inclusion of any entropic contribution. The Gibbs energy of this adduct in the gas phase is calculated to be more than 20.7 kcal mol^{-1} above the Gibbs energy of the separated reactants. This value is most likely too high, but there is no doubt that coordination of H_2 to give the σ-complex is not energetically favorable. Therefore, the Ir−O d_π-p_π interaction responsible for the DTBP geometry of **1** must be stronger than the interaction of H_2 with the metal center.

dx.doi.org/10.1021/ic301601c | *Inorg. Chem.* 2012, 51, 12313−12323

The proton transfer from **1·H$_2$** to **7-T** is accompanied by a gradual increase in the Ir−O bond length and proceeds via a transition state **1·H$_2$-TS** (Figure 9, center) calculated to be 18 kcal mol^{-1} above the separated cation **1** and H$_2$ (the associated Gibbs activation energy under standard conditions is 27.5 kcal mol^{-1}). The formation of the product **7-T** is exoenergetic by 8.9 kcal mol^{-1} relative to the separated reactants **1** and H$_2$; however, the inclusion of the entropic correction shows that the formation of **7-T** is marginally endoergic (ΔG = 4.8 kcal mol^{-1}). These values illustrate that the hydrogenation of **1** is likely to be slow and that the monomeric products of the reaction are thermodynamically unstable. However, the presence of a protic hydrogen atom in **7** allows for a stabilizing interaction with a hydrogen bond accepting solvent, which may be responsible for the strong solvent dependence of the reaction seen experimentally.

DISCUSSION

Complex **1**[**PF$_6$**] is a coordinatively unsaturated Ir^{III} alkoxide that reacts reversibly with a number of Lewis bases and with hydrogen. The reversibility of Lewis base binding, particularly in the case of methanol and acetonitrile, is likely related to the stability of **1** versus the saturated 18e$^-$ adducts. The methanol adduct [**1·MeOH**]**PF$_6$** is of special interest because by analogy, water should also be able to bind in the same manner. It was previously postulated that ionization of the chloride anion of the neutral 18e$^-$ complex **1**[**Cl**] in dilute aqueous solution would create a vacant site on the metal and allow formation of an aqua complex;[27] however, based on the results reported here it is likely that the chloro and aqua species are also in equilibrium with an unsaturated 16 e$^-$ form in aqueous solution. The speciation of such solutions may be further complicated by the presence of the chloride-bridged dimer **5** or an isostructural dimer with a hydroxide bridge.

In contrast to the solvent adducts, the carbonyl complex **2** shows interesting behavior by ^{1}H NMR. While CO binding is clearly reversible, the geminal methyl groups of the pyridylpropanolate ligand are inequivalent, suggesting that chemical exchange between **1** and **2** is slow. For the chloro complex **1**[**Cl**][27] a single broad resonance is seen in acetone-d$_6$ indicating that while CO loss from **2** is facile, the exchange process is substantially slower than chloride exchange between **1**[**Cl**] and [**1**]$^+$Cl$^-$ in acetone. The lability of chloride and CO in these compounds is atypical for Cp*Ir complexes and can likely be attributed to the labilizing influence of the alkoxide ligand.[5]

In reactions of **1**[**PF$_6$**] with substrates having protic hydrogen atoms, products typically exhibit strong intramolecular hydrogen bonds manifesting as a short O···O distance in the solid state and a far downfield-shifted resonance in the ^{1}H NMR spectrum. Both acetic acid and acetophenone oxime can serve as ligands while also adopting a geometry which allows for intramolecular hydrogen bonding with the pyridylpropanolate ligand. Oximes frequently form strong intramolecular hydrogen bonds in the secondary coordination sphere in transition metal glyoxime complexes, and this motif also appears in the acetophenone oxime adduct **3**.

Hydrogen bonds of this type can be classified based on their donor−acceptor distance, with the strongest hydrogen bonds being symmetrical or nearly so. These typically arise from the interaction of charged donors or acceptors and have significant three-center four-electron covalent bonding character.[18,26] The size of the ring formed by the acetate bridge between the iridium and oxygen atom of the pyridylpropanolate ligand in **4** does not appear to significantly affect the O···O distance, as the previously reported cocrystal of **1**[**Cl**] and acetic acid has a comparably short O···O distance of 2.459(3).[27]

The stabilizing effect of intramolecular hydrogen bonding in these complexes is perhaps most clearly evident in the chloride and hydride bridged dimeric complexes **5** and **6**. The computational data and the very short O···O distances in the X-ray crystal structures suggest that these interactions may be near-symmetrical hydrogen bonds. From the X-ray data, there is sufficient electron density in the difference map to refine the hydrogen atom positions in both **5** and **6** without restraint, and in both cases the refined H-atom position is consistent with a near-symmetrical hydrogen bond. The OH stretching band in these dimeric complexes could not be located in the FTIR spectra. Strong hydrogen bonds where the oxygen atoms are separated by less than 2.5 Å typically show low intensity IR bands that occur below 800 cm^{-1} such that the corresponding bands in deuterium labeled molecules are beyond the reach of most IR instruments.[18]

Calculations on **5** support this description of the intramolecular hydrogen bond. The precise location of the hydrogen atom cannot be calculated with certainty because the potential energy surface associated with the hydrogen position is very flat.[52] The O···O distance is in a range that leads to a very shallow energy barrier for proton transfer between the two oxygen atoms, calculated to be approximately 1.4 kcal mol^{-1}. A slight shortening of the O···O distance would shift the energy profile to one with a single minimum and a symmetrical hydrogen bond. On the basis of the calculations it is difficult to distinguish which is the best description for **5**, with the proton being either delocalized between the two oxygen atoms in a low-barrier hydrogen bond or in a symmetrical position between the two oxygens. In the case of complex **6**, the shorter intramolecular O···O distance favors the latter description of a single symmetrical minimum. Thus the position of the proton clearly depends strongly on the distance between the two oxygen atoms.

Gas phase calculations are found to describe the structural features and ^{1}H chemical shifts of **1**−**6** in good agreement with experimental values. Inclusion of either explicit anions or a solvent continuum model does not improve the results at this level of theory. The minimized structures are consistent with previous computational studies that show that as the distance between the two oxygens decreases, the hydrogen bond becomes more symmetrical. Accordingly, the deshielding of the proton increases as the distance between the two oxygen atoms shortens. These results extend previous computational studies of strong hydrogen bonds to a transition metal−supported system.[21−26]

In light of the large solvent dependence on the addition of hydrogen to **1**[**PF$_6$**] to give either **6** or the monomer **7**, it is likely that the reaction is mediated to a large extent by hydrogen bonding in the products. No addition is observed in certain strongly coordinating solvents, and the monomeric product **7** is not observed in methylene chloride. The addition is envisioned to occur via initial formation of a dihydrogen complex **1·H$_2$** which is deprotonated by the pendant alkoxide to give **7**, which can be trapped by another equivalent of **1**[**PF$_6$**] to give **6**.[53] Deprotonation of **1·H$_2$** by a second equivalent of **1**[**PF$_6$**] is less likely, as the loss of the d_π-p_π interaction in **1·H$_2$** on H$_2$ coordination can be expected to increase the basicity of the pendant alkoxide relative to **1**[**PF$_6$**]. In the absence of a

suitable hydrogen bond-accepting solvent such as dimethylformamide (DMF), partial hydrogenation to **6** appears to be preferred over complete conversion to **7**, which may be the result of a thermodynamic preference for **6** in the absence of an H-bond accepting solvent. Calculations on H_2 addition to **1** are consistent with initial formation of an unstable σ-complex followed by proton transfer to give the monomeric product **7**, the net formation of which may be endoergic and not favored in the absence of solvent stabilization. Under conditions which allow for the observation of **7** by ^{1}H NMR, its tendency to react with excess hydrogen to give over-reduced products and to lose hydrogen to give **6** has precluded its isolation in the solid state. However, the formation of **6** and **7** as products of hydrogenation of **1**[PF_6] clearly demonstrates the net addition of H_2 across a formal iridium−oxygen π bond and the importance of hydrogen bonding in stabilizing the resulting products.

The geometry and electronic structure of the hydride-bridged dimeric complex **6** are especially notable for their relevance to a key step in outer sphere hydrogen transfer. Noyori-type outer sphere hydrogenation involves the concerted transfer of a hydride and a proton between a bifunctional catalyst and the substrate as shown in Scheme 5, although

Scheme 5. Schematic Representation of Outer Sphere Hydrogenation

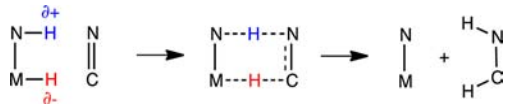

computations have also shown the active role of a protic solvent.[54] Like the proposed Noyori transition state, complex **6** includes protic and hydridic hydrogen atoms in a six-membered ring containing a hydrogen-donating metal-heteroatom pair and an accepting atom pair, in this case another metal and heteroatom. Complex **6** can therefore be viewed as an isolable model complex with analogy to the proposed Noyori transition state for outer sphere hydrogenation. Models of arrested transition states have been used to support proposed reaction mechanisms dating back to the important early work of Bürgi and Dunitz.[55] The pathway for C−H oxidative addition to a metal fragment was later analyzed in the same way by Crabtree et al.[56] In the present case, the fact that **6** resembles the OS hydrogenation transition state is qualitatively consistent with the idea that the Noyori transition state is of relatively low energy and that concerted outer sphere hydrogenation should be accessible with bifunctional metal-alcohol catalysts.

CONCLUSION

Cp* iridium complexes supported by the 2-(2′-pyridyl)-2-propanolate ligand display enhanced lability in ligand exchange reactions because of the influence of the oxygen π electrons which destabilize the octahedral geometry relative to a distorted trigonal bipyramidal geometry containing a formal iridium−oxygen double bond. The basicity of the alkoxide ligand has been demonstrated by its tendency to form strong, symmetrical or near-symmetrical intramolecular hydrogen bonds that result in very short O···O distances (2.39−2.45 Å). DFT calculations on the cationic metal species give structural parameters in excellent agreement with the values observed in the solid state structures. The unsaturated complex **1**[PF_6] reacts with hydrogen in a formal addition of H_2 across the iridium−oxygen π bond to give an observable monomeric iridium hydride with a protonated ligand (**7**) and an isolable dimer (**6**) resulting from trapping of the monomer by a second equivalent of **1**[PF_6]. This reaction is predicted to be endoergic by DFT and is observed to be solvent dependent, which implicates hydrogen bonding as a stabilizing interaction in the hydrogenation of **1**[PF_6]. The hydride-bridged dimer **6** has the shortest O···H···O hydrogen bond in the family complexes analyzed with an O···O distance of 2.392(9) Å. DFT calculations on **6** and the related chloride-bridged dimer **5** support a description of these interactions as symmetrical or nearly symmetrical hydrogen bonds. The proton and hydride bridged dimer **6** can be viewed as a model for the transition state in a key step of outer-sphere hydrogenation.

EXPERIMENTAL SECTION

General Procedures. ^{1}H NMR spectra were collected on a 400 MHz Bruker spectrometer and referenced to the residual protio-solvent signal. ^{13}C NMR spectra were collected on a 500 MHz Varian spectrometer and referenced to the solvent ^{13}C signal. δ is reported in units of parts per million (ppm) and J in hertz (Hz). Elemental analyses were performed by Atlantic Microlab, Inc. 2-(2′-Pyridyl)-2-propanol[57] and [Cp*$IrCl_2$]$_2$[58] were obtained according to published procedures.

(η^5-C_5Me_5)Ir(2-(2′-pyridyl)-2-propanolate)PF_6 (1[PF_6]). [Cp*$IrCl_2$]$_2$ (0.2045 g, 0.2567 mmol), Na_3PO_4·12H_2O (0.658 g, 1.73 mmol), KPF_6 (0.300 g, 1.63 mmol), and 2-(2′-pyridyl)-2-propanol (0.0710 g, 0.518 mmol) were combined in a 50 mL beaker and 15 mL of deionized water was added. The mixture was stirred in air for three to five minutes, until the colorless phosphate salts had largely dissolved, and then 15 mL of dichloromethane was added. The biphasic mixture was stirred vigorously for 10 min and then transferred to a separatory funnel. The organic layer was separated and the aqueous layer returned to the beaker with a fresh 15 mL portion of methylene chloride. After 10 min the second organic layer was separated and the two organic portions were combined, dried over anhydrous Na_2SO_4, and reduced to dryness on a rotary evaporator. The resulting solid was washed with 30 mL of diethyl ether and dried in vacuo to give the product as a red solid. Yield 0.231 g (74%). ^{1}H NMR (500 MHz, MeOD-d_4) δ 9.02 (d, J = 5.7 Hz, 1H), 8.08 (t, J = 7.9 Hz, 1H), 7.72 (d, J = 7.9 Hz, 1H), 7.57 (t, J = 6.3 Hz, 1H), 1.77 (s, 15H), 1.53 (s, 6H). ^{13}C{^{1}H} NMR (126 MHz, MeOD-d_4) δ 178.94, 151.69, 141.54, 126.29, 123.33, 88.83, 88.27, 32.11, 9.45. Calcd for $C_{18}H_{25}IrNOPF_6$: C, 35.52; H, 4.14; N, 2.30. Found: C, 35.07; H, 4.16; N, 2.27. Crystal samples used for X-ray crystallography were obtained by slow diffusion of diethyl ether into a concentrated methylene chloride solution.

(η^5-C_5Me_5)Ir(2-(2′-pyridyl)-2-propanolate)BPh_4 (1[BPh_4]). [Cp*$IrCl_2$]$_2$ (0.2049 g, 0.2572 mmol), Na_3PO_4·12H_2O (0.738 g, 1.94 mmol), and 2-(2′-pyridyl)-2-propanol (0.0726 g, 0.529 mmol) were combined in a 50 mL beaker and 10 mL of deionized water was added. The mixture was stirred in air for ten minutes, and then 20 mL of dichloromethane was added. The biphasic mixture was stirred vigorously for 5 min and then $NaBPh_4$ (0.2650 g, 0.7744 mmol) was added along with an additional 10 mL portion of water. The addition of the borate salt was accompanied by a change in the color of the organic layer to deep red. After stirring an additional 10 min the organic phase was separated in a separatory funnel, then dried over anhydrous Na_2SO_4 and reduced to dryness on a rotary evaporator. The resulting solid was washed with 30 mL of diethyl ether and dried in vacuo to give the product as a pink solid. Yield 0.300 g (75%). ^{1}H NMR (400 MHz, CD_2Cl_2) δ 8.82 (d, J = 5.7 Hz, 1H), 7.91 (td, J = 7.9, 1.5 Hz, 1H), 7.62 (d, J = 8.0 Hz, 1H), 7.38 (ddd, J = 7.4, 5.9, 1.4 Hz, 1H), 7.35−7.25 (m, 8H), 7.02 (t, J = 7.4 Hz, 8H), 6.86 (t, J = 7.2 Hz, 4H), 1.79 (s, 15H), 1.51 (s, 6H). ^{13}C{^{1}H} NMR (126 MHz, CD_2Cl_2) δ 181.05, 165.16, 164.77, 164.38, 163.99, 150.81, 141.11, 136.47, 126.15, 125.62, 122.39, 122.26, 93.09, 89.60, 31.12, 10.43. Calcd for $C_{42}H_{45}BIrNO$: C, 64.44; H, 5.79; N, 1.79. Found: C, 64.20; H, 5.89;

dx.doi.org/10.1021/ic301601c | Inorg. Chem. 2012, 51, 12313−12323

N, 1.86. Crystal samples used for X-ray crystallography were obtained by slow diffusion of diethyl ether into a concentrated methylene chloride solution.

(η^5-C_5Me_5)Ir(2-(2′-pyridyl)-2-propanolate)CO(PF_6) (2). A Schlenk flask was charged with **1**[PF_6] (0.0522 g, 0.0858 mmol) and 3 mL of methanol and degassed by sparging with argon. The solution was then sparged with CO gas for 5 min at room temperature, rapidly changing color to yellow. Removal of the solvent in vacuo gave the product as a yellow solid. Yield 0.0332 g (61%). The product is stable in the solid state but loses CO on standing in solution. ^{1}H NMR (500 MHz, MeOD-d_4) δ 8.58 (d, J = 5.8 Hz, 1H), 8.15 (t, J = 7.9 Hz, 1H), 7.58−7.53 (m, 2H), 1.91 (s, 15H), 1.55 (s, 3H), 1.43 (s, 3H). ^{13}C{^{1}H} NMR (126 MHz, MeOD-d_4) δ 177.57, 171.04, 152.56, 142.71, 127.47, 124.45, 102.94, 87.80, 32.75, 31.15, 8.81. ν(CO) = 2038.8 cm^{-1}. Calcd for $C_{19}H_{23}F_6IrNO_2P$: C, 35.85; H, 3.96; N, 2.20. Found: C, 35.72; H, 4.35; N, 2.29. Crystal samples used for X-ray crystallography were obtained by layering diethyl ether onto a concentrated methanol solution under a mixed atmosphere of nitrogen and carbon monoxide.[59]

(η^5-C_5Me_5)Ir(2-(2′-pyridyl)-2-propanolate)(acetophenone oxime)PF_6 (3). Acetophenone oxime (0.0109 g, 0.0806 mmol) and **1**[PF_6] (0.0452 g, 0.0743 mmol) were combined in a 10 mL round-bottom flask in air with an attached reflux condenser and treated with 4 mL of ethyl acetate. The suspension was heated to reflux for 5 min in a hot water bath with vigorous stirring, and then allowed to slowly cool back to room temperature without stirring. The flask was then capped and transferred to the freezer for an hour. Filtration in air gave the product as a yellow microcrystalline solid which was washed with 10 mL of diethyl ether and dried in vacuo. Yield 0.0382 g (69%). ^{1}H NMR (500 MHz, CD_2Cl_2) δ 14.94 (s, br, 1H), 8.43 (dt, J = 5.7, 0.8 Hz, 1H), 8.05−7.99 (m, 1H), 7.63−7.48 (m, 4H), 7.39−7.35 (m, 1H), 7.02−6.98 (m, 2H), 2.55 (s, 3H), 1.53 (s, 6H), 1.32 (s, 15H). ^{13}C{^{1}H} NMR (126 MHz, CD_2Cl_2) δ 177.11, 165.89, 151.21, 140.39, 137.12, 131.07, 129.56, 128.90, 125.76, 123.31, 88.01, 85.17, 32.36, 21.72, 8.92. Crystal samples used for X-ray crystallography were obtained by a modification of this preparation. Additional ethyl acetate was added to the refluxing solution until the solution was entirely homogeneous prior to removal from the heat source. This modification reduces the yield from the first crystallization but gives large crystals.

(η^5-C_5Me_5)Ir(2-(2′-pyridyl)-2-propanol)(acetate)PF_6 (4). A solution of acetic acid (0.5 mL) in 3 mL of methylene chloride was added to **1**[PF_6] (0.0382 g, 0.0628 mmol) in a 50 mL round-bottom flask in air and stirred for 15 min. The stir bar was removed and 25 mL of diethyl ether was carefully layered on top of the methylene chloride solution and the flask capped. After standing at room temperature for approximately 6 h, a large number of yellow crystals had deposited. The flask was then stored overnight in the freezer, and the crystals collected by vacuum filtration of the cold suspension, followed by washing with 10 mL of diethyl ether. Yield 0.0292 g (70%). ^{1}H NMR (400 MHz, CD_2Cl_2, 25 °C) δ 8.72 (d, J = 5.5 Hz, 1H), 8.05 (td, J = 7.8, 1.5 Hz, 1H), 7.61 (ddd, J = 7.5, 5.7, 1.4 Hz, 1H), 7.46 (d, J = 8.0 Hz, 1H), 1.88 (s, 3H), 1.63 (s, 15H), 1.58 (s, 6H). ^{1}H NMR (400 MHz, CD_2Cl_2, −60 °C) δ 15.77 (1H), 8.65 (1H), 8.02 (1H), 7.57 (1H), 7.41 (1H), 1.82 (3H), 1.68 (3H), 1.54 (15H), 1.31 (3H). ^{13}C{^{1}H} NMR (126 MHz, CD_2Cl_2, 25 °C) δ 186.62, 169.71, 150.48, 141.58, 126.94, 122.59, 87.14, 84.95, 29.26, 25.21, 9.35. Anal. Calcd for $C_{20}H_{29}F_6IrNO_3P$: C, 35.93; H, 4.37; N, 2.09. Found: C, 35.69; H, 4.56; N, 2.17.

[(η^5-C_5Me_5)Ir(2-(2′-pyridyl)-2-propanolate)]$_2$HCl(PF_6)$_2$ (5). Freshly prepared diphenylammonium chloride (0.0038 g, 0.018 mmol) and **1**[PF_6] (0.0212 g, 0.0348 mmol) were combined in the dark[60] in 2 mL of dichloromethane in air and stirred 30 min. The stir bar was then removed, and 5 mL of diethyl ether was carefully layered on top and the flask capped. Yellow crystals deposited from the solution on standing overnight and were collected by vacuum filtration and washed with 5 mL of toluene. Yield 0.0143 g (66%). ^{1}H NMR (500 MHz, CD_2Cl_2, 25 °C) δ 8.71 (d, J = 5.4 Hz, 2H), 8.09 (td, J = 7.9, 1.2 Hz, 2H), 7.65 (t, J = 6.8 Hz, 2H), 7.58 (d, J = 8.0 Hz, 2H), 1.61 (s, br, 12H), 1.40 (s, 30H). ^{1}H NMR (400 MHz, CD_2Cl_2, −20 °C) δ 14.24 (s, br, 1H), 8.66 (d, J = 5.9 Hz, 2H), 8.08 (td, J = 7.7, 1.3 Hz, 2H), 7.63 (ddd, J = 7.0, 5.9, 1.0 Hz, 2H), 7.55 (d, J = 8.1 Hz, 2H), 1.83 (s, 6H), 1.26 (s, 36H). ^{13}C{^{1}H} NMR (126 MHz, CD_2Cl_2) δ 170.42, 151.23, 141.71, 127.02, 122.27, 88.91, 85.67, 30.47, 9.53. Anal. Calcd for $C_{36}H_{51}ClF_{12}Ir_2N_2O_2P_2$: C, 34.49; H, 4.10; N, 2.23. Found: C, 34.25; H, 4.31; N, 2.21. Crystal samples used for X-ray crystallography were obtained either by this preparation or by slow diffusion of diethyl ether into a concentrated methylene chloride solution.[61]

[(η^5-C_5Me_5)Ir(2-(2′-pyridyl)-2-propanolate)]$_2$$H_2$($PF_6$)$_2$ (6). A Schlenk flask was charged with **1**[PF_6] (0.0335 g, 0.0550 mmol) and 4 mL of methanol and degassed by sparging with argon. The solution was cooled to −30 °C and then sparged with H_2 gas for 2 min. The flask was then warmed to −20 °C and allowed to stand under H_2 for 15 min. The bath was then warmed to 0 °C, and the flask evacuated to dryness to yield the product as a red-orange solid. Yield 0.0186 g (55%). ^{1}H NMR (400 MHz, CD_2Cl_2, −60 °C) δ 16.25 (s, 1H), 8.80 (d, J = 5.5 Hz, 2H), 8.00 (t, J = 7.9 Hz, 2H), 7.75 (t, J = 6.7 Hz, 2H), 7.42 (d, J = 8.1 Hz, 2H), 1.72 (s, 6H), 1.29 (s, 30H), 1.26 (s, 6H), −15.32 (s, 1H). Crystal samples used for X-ray crystallography were obtained by layering toluene on a cold DMF solution of **1**[PF_6] which had been sparged with H_2. The product is unstable in solution above −20 °C, but stable in the solid state for weeks in air at room temperature. The instability of this complex in solution at room temperature precluded the collection of ^{13}C NMR data. Anal. Calcd for $C_{36}H_{52}F_{12}Ir_2N_2O_2P_2$: C, 35.47; H, 4.30; N, 2.30. Found: C, 35.29; H, 4.20; N, 2.30.

Computational Details. All calculations were performed with the Gaussian09 package[62] of programs with the hybrid B3PW91 functional,[63,64] and with hybrid B3PW91-D functional corrected with dispersion.[65] Iridium was represented with the quasi-relativistic effective core potential (RECP) from the Stuttgart group and the associated basis set[66] augmented by an f polarization function.[67] The phosphorus and chlorine were represented by RECPs from the Stuttgart group and the associated basis set,[68] augmented by a d polarization function.[69] A 6-31G(d,p) basis set was used for all the other atoms (H, C, N, O, F).[70] For the NMR calculations, Ir, Cl, and P were represented with the RECP and basis sets used for the geometry optimization, and H, C, N, O, F were represented by a pc-2 basis set proposed by Jensen.[71,72] The geometry optimizations were performed without any symmetry constraint followed by analytical frequency calculations. The nature of the extrema (minimum or transition state) was verified by the analytical calculation of the frequencies. The connection between transition state and minima was verified by Intrinsic Reaction calculations (IRC). The Gibbs energies were calculated assuming an ideal gas, unscaled harmonic frequencies, and the rigid rotor approximation in the standard conditions (p = 1 atm and T = 298 K). The IR frequencies were calculated within the harmonic approximation and were not scaled. The ^{1}H NMR chemical shift was computed with the GIAO[73] method available in the Gaussian09 program.

■ ASSOCIATED CONTENT

Ⓢ Supporting Information

Details of the X-ray crystallographic analysis of **1**[PF_6], **1**[BPh_4], [**1**·MeOH]PF_6, **2**, **3**, **4**, **5**, **6**, and 2-(2′-pyridyl)-2-propanol. ^{1}H and ^{13}C{^{1}H} NMR spectra, FTIR spectrum of **2**, and the full list of authors for reference 62, and Cartesian coordinates of all optimized structures and corresponding energies in a.u. This material is available free of charge via the Internet at http://pubs.acs.org.

■ AUTHOR INFORMATION

Corresponding Author

*E-mail: robert.crabtree@yale.edu.

Notes

The authors declare no competing financial interest.

■ ACKNOWLEDGMENTS

This material is based upon work supported by the U.S. Department of Energy, Office of Science, Office of Basic Energy Sciences Catalysis Program under Award Number DE-FG02-84ER13297. C.R. and O.E. thank the CNRS and the Ministère de l'Enseignement Supérieur et de la Recherche (MESR) for funding. S.H. thanks the MESR for a Ph.D. Fellowship.

■ REFERENCES

(1) Bradley, D. C. *Alkoxo and aryloxo derivatives of metals*; Academic Press: San Diego, CA, 2001.
(2) Cantalupo, S. A.; Lum, J. S.; Buzzeo, M. C.; Moore, C.; DiPasquale, A. G.; Rheingold, A. L.; Doerrer, L. H. *Dalton Trans.* **2010**, *39*, 374.
(3) Bryndza, H. E.; Tam, W. *Chem. Rev.* **1988**, *88*, 1163.
(4) Fulton, J. R.; Holland, A. W.; Fox, D. J.; Bergman, R. G. *Acc. Chem. Res.* **2001**, *35*, 44.
(5) Caulton, K. G. *New J. Chem.* **1994**, *18*, 25.
(6) Brunner, H.; Muschiol, M.; Tsuno, T.; Takahashi, T.; Zabel, M. *Organometallics* **2008**, *27*, 3514.
(7) Johnson, T. J.; Huffman, J. C.; Caulton, K. G. *J. Am. Chem. Soc.* **1992**, *114*, 2725.
(8) Johnson, T. J.; Folting, K.; Streib, W. E.; Martin, J. D.; Huffman, J. C.; Jackson, S. A.; Eisenstein, O.; Caulton, K. G. *Inorg. Chem.* **1995**, *34*, 488.
(9) Balogh, J.; Slawin, A. M. Z.; Nolan, S. P. *Organometallics* **2012**, *31*, 3259.
(10) Gemel, C.; Sapunov, V. N.; Mereiter, K.; Ferencic, M.; Schmid, R.; Kirchner, K. *Inorg. Chim. Acta* **1999**, *286*, 114.
(11) Glueck, D. S.; Wu, J. X.; Hollander, F. J.; Bergman, R. G. *J. Am. Chem. Soc.* **1991**, *113*, 2041.
(12) Samec, J. S. M.; Bäckvall, J. E.; Andersson, P. G.; Brandt, P. *Chem. Soc. Rev.* **2006**, *35*, 237.
(13) Abdur-Rashid, K.; Clapham, S. E.; Hadzovic, A.; Harvey, J. N.; Lough, A. J.; Morris, R. H. *J. Am. Chem. Soc.* **2002**, *124*, 15104.
(14) Clapham, S. E.; Hadzovic, A.; Morris, R. H. *Coord. Chem. Rev.* **2004**, *248*, 2201.
(15) Comas-Vives, A.; Ujaque, G.; Lledós, A. Inner- and Outer-Sphere Hydrogenation Mechanisms: A Computational Perspective. In *Advances in Inorganic Chemistry*; van Eldik, R., Harvey, J., Eds.; Academic Press: Orlando, FL, 2010; Vol. *62*, p 231.
(16) Renkema, K. B.; Huffman, J. C.; Caulton, K. G. *Polyhedron* **1999**, *18*, 2575.
(17) Bullock, R. M. *Chem.—Eur. J.* **2004**, *10*, 2366.
(18) Gilli, G.; Gilli, P. *J. Mol. Struct.* **2000**, *552*, 1.
(19) Jeffrey, G. A.; Saenger, W. *Hydrogen bonding in biological structures*; Springer-Verlag: Berlin, Germany, 1994.
(20) Landrum, G. A.; Goldberg, N.; Hoffmann, R. *J. Chem. Soc., Dalton Trans.* **1997**, 3605.
(21) Garcia-Viloca, M.; Gelabert, R.; Gonzalez-Lafont, A.; Moreno, M.; Lluch, J. M. *J. Phys. Chem. A* **1997**, *101*, 8727.
(22) Garcia-Viloca, M.; Gonzalez-Lafont, A.; Lluch, J. M. *J. Am. Chem. Soc.* **1997**, *119*, 1081.
(23) Kumar, G. A.; McAllister, M. A. *J. Org. Chem.* **1998**, *63*, 6968.
(24) Chen, J. G.; McAllister, M. A.; Lee, J. K.; Houk, K. N. *J. Org. Chem.* **1998**, *63*, 4611.
(25) Kumar, G. A.; McAllister, M. A. *J. Am. Chem. Soc.* **1998**, *120*, 3159.
(26) Grabowski, S. J. *Chem. Rev.* **2011**, *111*, 2597.
(27) Schley, N. D.; Blakemore, J. D.; Subbaiyan, N. K.; Incarvito, C. D.; D'Souza, F.; Crabtree, R. H.; Brudvig, G. W. *J. Am. Chem. Soc.* **2011**, *133*, 10473.
(28) Holland, A. W.; Glueck, D. S.; Bergman, R. G. *Organometallics* **2001**, *20*, 2250.
(29) Holland, A. W.; Bergman, R. G. *Inorg. Chim. Acta* **2002**, *341*, 99.
(30) Hou, Z.; Fujita, A.; Koizumi, T.-a.; Yamazaki, H.; Wakatsuki, Y. *Organometallics* **1999**, *18*, 1979.
(31) There are 24 iridium alkoxide structures in the Cambridge Structural Database (2011) with Ir-O bond lengths of less than 2.0 Å, including acetylacetonates
(32) Arita, S.; Koike, T.; Kayaki, Y.; Ikariya, T. *Organometallics* **2008**, *27*, 2795.
(33) Zhang, G.; Wen, X.; Wang, Y.; Mo, W.; Ding, C. *J. Org. Chem.* **2011**, *76*, 4665.
(34) Madabhushi, S.; Chinthala, N.; Vangipuram, V. S.; Godala, K. R.; Jillella, R.; Mallu, K. K. R.; Beeram, C. R. *Tetrahedron Lett.* **2011**, *52*, 6103.
(35) Kashiwame, Y.; Kuwata, S.; Ikariya, T. *Chem.—Eur. J.* **2010**, *16*, 766.
(36) Shvo, Y.; Czarkie, D.; Rahamim, Y.; Chodosh, D. F. *J. Am. Chem. Soc.* **1986**, *108*, 7400.
(37) Tse, S. K. S.; Xue, P.; Lau, C. W. S.; Sung, H. H. Y.; Williams, I. D.; Jia, G. *Chem.—Eur. J.* **2011**, *17*, 13918.
(38) Dahlenburg, L.; Treffert, H.; Farr, C.; Heinemann, F. W.; Zahl, A. *Eur. J. Inorg. Chem.* **2007**, *2007*, 1738.
(39) Vaartstra, B. A.; Huffman, J. C.; Gradeff, P. S.; Hubert-Pfalzgraf, L. G.; Daran, J. C.; Parraud, S.; Yunlu, K.; Caulton, K. G. *Inorg. Chem.* **1990**, *29*, 3126.
(40) Geometry optimization with a DFT-D method gives a minimum with a symmetric hydrogen bond but the geometry of the dinuclear dication is in poorer agreement with the experimental structure. Notably, the calculated O···O distance is too short.
(41) As mentioned earlier, test calculations introducing the PF_6^- anion did not lead to any significant lowering of the ^1H chemical shift.
(42) The bridging hydride was not located in the difference map, but was instead placed at an idealized location and refined with restraints placed on the two Ir-H distances. See Supporting Information for details.
(43) Royer, A. M.; Rauchfuss, T. B.; Gray, D. L. *Organometallics* **2010**, *29*, 6763.
(44) Yamaguchi, R.; Ikeda, C.; Takahashi, Y.; Fujita, K. *J. Am. Chem. Soc.* **2009**, *131*, 8410.
(45) Kang, J. W.; Maitlis, P. M. *J. Organomet. Chem.* **1971**, *30*, 127.
(46) White, C.; Gill, D. S.; Kang, J. W.; Lee, H. B.; Maitlis, P. M. *J. Chem. Soc., Chem. Commun.* **1971**, 734.
(47) White, C.; Oliver, A. J.; Maitlis, P. M. *J. Chem. Soc., Dalton Trans.* **1973**, 1901.
(48) Gill, D. S.; Maitlis, P. M. *J. Organomet. Chem.* **1975**, *87*, 359.
(49) Gilbert, T. M.; Bergman, R. G. *Organometallics* **1983**, *2*, 1458.
(50) del Rosa, I.; Jolibois, F.; Maron, L.; Philippot, K.; Chaudret, B.; Poteau, R. *Dalton Trans.* **2009**, 2142.
(51) Hrobárik, P.; Hrobáriková, V.; Meier, F.; Repiský, M.; Komorovský, S.; Kaupp, M. *J. Phys. Chem. A* **2011**, *115*, 5654.
(52) Maseras, F.; Lledós, A.; Clot, E.; Eisenstein, O. *Chem. Rev.* **2000**, *100*, 601.
(53) Attempts to determine if DMF assists in deprotonation of the H_2 adduct of **1** did not yield good results. It appears that the combined effect of solvent and counterion is difficult to represent in this study.
(54) Eisenstein, O.; Crabtree, R. H. *New J. Chem.* **2013**, DOI: 10.1039/c2nj40659d and references therein. Handgraaf, J.-W.; Meijer, E. J. *J. Am. Chem. Soc.* **2007**, *129*, 3099.
(55) Bürgi, H. B.; Dunitz, J. D. *Acc. Chem. Res.* **1983**, *16*, 153.
(56) Crabtree, R. H.; Holt, E. M.; Lavin, M.; Morehouse, S. M. *Inorg. Chem.* **1985**, *24*, 1986.
(57) Wong, Y.-L.; Yang, Q.; Zhou, Z.-Y.; Lee, H. K.; Mak, T. C. W.; Ng, D. K. P. *New J. Chem.* **2001**, *25*, 353.
(58) Koelle, U.; Kossakowski, J.; Grumbine, D.; Tilley, T. D. *Inorg. Synth.* **1992**, *29*, 225.
(59) During the course of this study two crystal polymorphs of this compound were found. Polymorph 1 (monohydrate) ($P2_1/c$), a = 8.5250(9), b = 20.792(2), c = 13.5964(14), α = 90°, β = 98.695(3)°, γ = 90°, volume = 2382.3(4). Polymorph 2 (anhydrous) ($P2_1/n$), a = 15.6433(3), b = 8.3326(2), c = 16.8599(12), α = 90°, β = 100.429(7)°, γ = 90°, volume = 2161.37(17).
(60) Diphenylamine and its hydrochloride salt are light sensitive in solution.

(61) During the course of this study two crystal polymorphs of this compound were found. Polymorph 1 ($C2/c$), a = 18.578(6), b = 20.340(6), c = 24.619(7), α = 90°, β = 112.035(8)°, γ = 90°, volume = 8623(4). Polymorph 2 ($P2_1/c$), a = 10.2859(13), b = 23.603(3), c = 17.763(2), α = 90°, β = 92.460(3)°, γ = 90°, volume = 4308.6(9).
(62) Frisch, M. J. et al. *GAUSSIAN 03*, revision C.02; Gaussian, Inc.: Wallingford, CT, 2004.
(63) Becke, A. D. *J. Chem. Phys.* **1993**, *98*, 5648.
(64) Perdew, J. P.; Wang, Y. *Phys. Rev. B* **1992**, *45*, 13244.
(65) Grimme, S.; Antony, J.; Ehrlich, S.; Krieg, H. *J. Chem. Phys.* **2010**, *132*, 154104.
(66) Andrae, D.; Häussermann, U.; Dolg, M.; Stoll, H.; Preuss, H. *Theor. Chim. Acta* **1990**, *77*, 123.
(67) Ehlers, A. W.; Böhme, M.; Dapprich, S.; Gobbi, A.; Höllwarth, A.; Jonas, V.; Köhler, K. F.; Stegmann, R.; Veldkamp, A.; Frenking, G. *Chem. Phys. Lett.* **1993**, *208*, 111.
(68) Bergner, A.; Dolg, M.; Küchle, W.; Stoll, H.; Preuss, H. *Mol. Phys.* **1993**, *80*, 1431.
(69) Höllwarth, A.; Böhme, M.; Dapprich, S.; Ehlers, A. W.; Gobbi, A.; Jonas, V.; Köhler, K. F.; Stegmann, R.; Veldkamp, A.; Frenking, G. *Chem. Phys. Lett.* **1993**, *208*, 237.
(70) Hariharan, P. C.; Pople, J. A. *Theor. Chim. Acta* **1973**, *28*, 213.
(71) Bunte, S. W.; Jensen, G. M.; McNesby, K. L.; Goodin, D. B.; Chabalowski, C. F.; Nieminen, R. M.; Suhai, S.; Jalkanen, K. J. *Chem. Phys.* **2001**, *265*, 13.
(72) Jensen, F. *J. Chem. Phys.* **2002**, *116*, 7372.
(73) Ditchfield, R. *Mol. Phys.* **1974**, *27*, 789.